Physics – Uspekhi **68** (3) 278 – 293 (2025)

PHYSICS OF OUR DAYS

PACS numbers: **07.87.+v, 95.55.–n, 96.55.+z**

Origin and transport of water in the Universe

M.S. Kirsanova, P.V. Baklanov, E.O. Vasiliev, A.I. Vasyunin, D.Z. Wiebe, S.A. Drozdov, T.I. Larchenkova, S.F. Likhachev, A.V. Moiseev, Ya.N. Pavlyuchenkov, P.S. Sozinova, A.P. Topchieva, I.V. Tret'yakov, G.S. Fedoseev, A.V. Khudchenko, N.N. Shakhvorostova

DOI: https://doi.org/10.3367/UFNe.2024.08.039744

Contents

Abstract. The origin and transport of water in the Universe are two of the key scientific programs for the Millimetron Space Observatory. This paper covers several astrochemical problems, from the formation of water in the local Universe to protoplanetary disks and comets. We discuss how to solve these problems with the Millimetron Space Observatory.

Keywords: submillimeter astronomy, molecules, galaxies, interstellar medium, protostars, disks, comets, water

M.S. Kirsanova [1,2,a], **P.V. Baklanov** [1,b], **E.O. Vasiliev** [1,c], **A.I. Vasyunin** [3], **D.Z. Wiebe** [2,5,d], **S.A. Drozdov** [1,e], **T.I. Larchenkova** [1,f], **S.F. Likhachev** [1,g], **A.V. Moiseev** [4,h], **Ya.N. Pavlyuchenkov** [2,i], **P.S. Sozinova** [1], **A.P. Topchieva** [2,j], **I.V. Tret'yakov** [1,k], **G.S. Fedoseev** [3,l], **A.V. Khudchenko** [1,m], **N.N. Shakhvorostova** [1,n]

[1] Astro Space Center, Lebedev Physical Institute, Russian Academy of Sciences, ul. Profsoyuznaya 84/32, 117810 Moscow, Russian Federation
[2] Institute of Astronomy, Russian Academy of Sciences, ul. Pyatnitskaya 48, 119017 Moscow, Russian Federation
[3] Ural Federal University named after the First President of Russia B.N. Yeltsin, prosp. Mira 19, 620002 Ekaterinburg, Russian Federation
[4] Special Astrophysical Observatory, Russian Academy of Sciences, Nizhnii Arkhyz, Zelenchukskiy region, Karachai-Cherkessian Republic, Russian Federation
[5] Lomonosov Moscow State University, Department of Chemistry, Leninskie gory 1, str. 2, 119991 Moscow, Russian Federation
E-mail: [a] kirsanova@inasan.ru, [b] baklanovp@lebedev.ru, [c] eugstar@mail.ru, [d] dwiebe@inasan.ru, [e] drozdovsa@lebedev.ru, [f] ltanya@asc.rssi.ru, [g] slikhach@asc.rssi.ru, [h] moisav@sao.ru, [i] pavyar@inasan.ru, [j] ATopchieva@inasan.ru, [k] tretyakoviv@lebedev.ru, [l] g.s.fedoseev@urfu.ru, [m] khudchenko@asc.rssi.ru, [n] nadya@asc.rssi.ru

Received 5 April 2024, revised 23 July 2024
Uspekhi Fizicheskikh Nauk **195** (3) 294 – 310 (2025)
Translated by A.I. Ulitkin

1. Introduction

"The Origin and Transport of Water in the Universe" is one of the key scientific programs for the Millimetron Space Observatory [1–3]. This program is aimed at determining the water content in various space objects from galaxies to comets, at studying mechanisms of water transfer between space objects of different types and the role of interstellar water molecules in the origins of life on Earth, and at investigating ways of water formation in the gas and solid phases of interstellar medium.

The most complete study of space objects and processes in the Universe requires measurements covering the entire electromagnetic spectrum. Most of this spectrum is hidden from ground-based telescopes by absorption in Earth's atmosphere, which is transparent to incoming light only in two relatively narrow windows: in the optical range (0.3–2 μm and partially up to 8 μm) and in the radio range (from 1 mm to 30 m). The opacity of the atmosphere at other wavelengths results from absorption and scattering of light by molecules and atoms. In particular, in the submillimeter wavelength range from 0.02 to 1 mm, absorption is due to oxygen molecules O_2, water vapor H_2O, and carbon dioxide CO_2, which are present in large quantities in Earth's atmosphere. This problem is partially solved by placing telescopes at high altitudes above sea level (or by launching airplanes and balloons), since the water vapor content decreases with altitude. However, the atmosphere does not become completely transparent to submillimeter radiation even at high altitudes, and so only space telescopes make it possible to fully realize the potential of observations in this range.

The water contained in Earth's atmosphere complicates ground-based observations of cosmic emission lines of this molecule, which is essential for biological evolution. Ground-based radio telescopes make it possible to observe only about ten water vapor emission lines, mainly maser lines, in the atmospheric transparency window region from 22 to

658 GHz. The most complete database of currently known water masers is published in [4]. Maser lines are nonthermal in nature and also arise in specific conditions of interstellar matter, which makes it difficult to determine the physical conditions in space objects with their help. Therefore, maser lines are used primarily to study the kinematics of medium and determine distances in the Galaxy [5–8] and beyond [9], and as indicators of nonstationary processes in evolved stars and protostellar objects [10, 11].

The vast majority of water emission lines are not accessible for observation using ground-based instruments. Space observatories with broadband radiation receivers (several terahertz) are capable of observing dozens of times more water lines. This, in turn, allows one to trace the chain of transformations and transfer of water in the interstellar medium (ISM) — from dense clouds to protoplanetary disks.

The Millimetron Space Observatory is the eighth space telescope (after ISO, SWAS, Odin, Spitzer, Herschel, SOFIA, and JWST observatories) to provide the technical ability to observe water vapor molecules in space objects. The Herschel telescope, significantly superior to its predecessors in both sensitivity and resolution, made it possible to trace the pathways of water formation in star-forming regions and showed how the main chains of reactions of water synthesis on the surface of dust particles and in the gas phase work. The telescope was also used to identify some objects in which water was formed through high-temperature and low-temperature reaction chains (see the review of the results in [12]). However, high competition regarding observation time within the framework of the water observation program on the Herschel telescope has made it impossible to move from studying individual objects to statistically significant samples. The uniform data obtained with the Herschel telescope are limited to the first survey of star-forming regions different masses at various stages of this process (from pre-stellar cores to main sequence stars with disks) in the lines of transition to the ground state of ortho- and para-water at 557 and 1113 GHz, respectively. In total, the survey included several dozen sources, which is clearly insufficient for statistically significant analysis. Observations in a wide frequency range from 557 to 2400 GHz using the HIFI heterodyne receiver and the PACS spectrograph yielded full spectral scans for only four sources.

The angular resolution of the Millimetron Space Observatory in the single-dish regime, almost three times higher than the angular resolution of the Herschel telescope, will allow compact regions from which water radiation emanates to be observed. In combination with higher sensitivity, this will make it possible to ensure a qualitative transition from fragmentary information about the water content in individual objects to identification of statistical patterns in the evolution of the water content in protostellar clouds, protoplanetary disks, and comets, thereby significantly approaching our understanding of how the conditions necessary for the emergence of life arise during the formation of planets.

2. High-resolution spectrometer of Millimetron Space Observatory

The Millimetron Space Observatory will operate in two modes — single-dish interferometer — to solve different scientific problems (see reviews [1–3]). The overwhelming majority of scientific problems within the program of studies on the origin and transport of water in the Universe will be solved thanks to observations in the single-dish regime using the onboard high-resolution spectrometer of the Millimetron Space Observatory, a detailed description of which is presented in Ref. [13]. This spectrometer will include heterodyne receivers for the following frequency ranges: 500–600 GHz, 750–900 GHz, 1080–1230 GHz, 1300–1400 GHz, 1890–1910 GHz, 2390–2410 GHz, and 2660–2680 GHz (Table 1). The proposed frequency ranges take into account the current technical capabilities for the implementation of onboard highly sensitive high-frequency resolution receivers [14]. The use of this wide-range instrument will allow a qualitative transition from fragmentary information about the content of water in individual objects to obtaining statistical patterns of its evolution.

In the first three ranges (M1–M3), use will be made of heterodyne receivers on superconductor–insulator–superconductor (SIS) mixers [15, 16]. These receivers successfully operate on leading submillimeter telescopes [17, 18] and are also installed aboard the Herschel space observatory [14]. The expected sensitivity indicators for this technology, expressed as the value of the system noise temperature T_n, are listed in Table 1. In this case, single-band noise temperature is presented. The given values of T_n are formulated taking into account the best indicators demonstrated for SIS receivers in the corresponding ranges [14, 19, 20]. The intermediate frequency band for receivers of the M1–M3 ranges will be assumed to be from 4 to 12 GHz. This means that, during

Table 1. Frequency ranges of the seven bands of Millimetron Space Observatory receiver, main spectral lines falling within these bands, number of receiver pixels, receiver temperature (T_n, K), and spatial resolution of the telescope in presented ranges (Θ, arc seconds).

No.	f, GHz	Main lines	Number of pixels	T_n, K (technology)	Θ, $''$
M1	500–600	Ortho-H_2O $1_{1.0}-1_{0.1}$ 556.9 Ortho-$H_2^{18}O$ $1_{1.0}-1_{0.1}$ 547.7 Ortho-$H_2^{17}O$ $1_{1.0}-1_{0.1}$ 552.0 HDO $1_{1.0}-1_{0.1}$ 509.3	3	200 (SIS)	14
M2	750–900	Para-H_2O $2_{1.1}-2_{0.2}$ 752.0 HDO $1_{1.1}-0_{0.0}$ 893.6 HDO $2_{1.2}-1_{1.1}$ 848.9	3	400 (SIS)	9
M3	1080–1230	Para-H_2O $1_{1.1}-0_{0.0}$ 1113.3 Para-$H_2^{18}O$ $1_{1.1}-0_{0.0}$ 1101.7 Para-$H_2^{17}O$ $1_{1.1}-0_{0.0}$ 1107.2 Para-H_2O $2_{2.0}-2_{1.1}$ 1228.8 Para-$H_2^{18}O$ $2_{2.0}-2_{1.1}$ 1199.1 Ortho-H_2O $3_{1.2}-3_{0.3}$ 1097.4 Ortho-H_2O $3_{1.2}-2_{2.1}$ 1153.1 Ortho-H_2O $3_{2.1}-3_{1.2}$ 1162.9 Para-H_2O $4_{2.2}-4_{1.3}$ 1207.6 Para-$H_2^{18}O$ $4_{2.2}-4_{1.3}$ 1188.9 Ortho-$H_2^{18}O$ $3_{1.2}-3_{0.3}$ 1095.6	3	1000 (SIS)	7
M4	1300–1400	Ortho-H_2O $6_{2.5}-5_{3.2}$ 1322.0 Para-H_2O $7_{4.4}-8_{1.7}$ 1344.7	7	1000 (HEB)	6
M5	1890–1910	CII $2P_{3/2}-2P_{1/2}$ 1900.5 ^{13}CII $2P_{3/2}-2P_{1/2}$ 1900.1–1900.9	7	1200 (HEB)	4
M6	2390–2410	Para-H_2O $4_{0.4}-3_{1.3}$ 2391.573 HDO $5_{3.3}-5_{2.4}$ 2399.218 Para-D_2O $6_{5.1}-6_{4.2}$ 2400.383	7	1400 (HEB)	3
M7	2660–2680	HD 1–0 2674.986	7	1400 (HEB)	3

observations, broadband spectra will be obtained in which, in addition to the main water lines, additional lines necessary for diagnosing physical conditions in the objects in question will be observed. At the same time, it is permissible to reduce the band to 4–8 GHz to save onboard resources, which will not have a critical impact on scientific tasks. The use of array receivers will increase the speed of mapping of extended objects. The diffraction limit, which decreases linearly with increasing frequency, determines the size of the pixels of the receiver array and affects the permissible number of pixels. The optical properties of the telescope allow either three pixels or seven pixels to be placed in focus for low-frequency M1–M3 ranges and higher-frequency receivers, respectively.

For the M4–M7 ranges operating at frequencies above 1300 GHz, use will be made of heterodyne array receivers based on a hot electron bolometer (HEB) [21]. The basis of the HEB sensitive element is a disordered thin superconducting film of niobium nitride NbN. The NbN HEB heterodyne receivers have successfully demonstrated their operation at the Herschel and SOFIA observatories. However, the sensitivity of NbN HEB mixers in these projects was far from the maximum possible. In heterodyne measurements, the sensitivity of the receiver is limited by quantum fluctuations of the heterodyne photons. The best value of the uncorrected two-sideband noise temperature of NbN HEB mixers, $T_{\rm n} = 600$ K, was obtained at a frequency of 2.52 THz [22], which corresponds to a single-sideband temperature of 1200 K. This value was taken to estimate the achievable sensitivity of the M4 and M5 instruments in Table 1. The planned intermediate frequency band for the M4–M7 receivers is 1–6 GHz. As a source of the heterodyne for the HEB, which requires a relatively high power, energy-optimized and frequency-stabilized quantum cascade lasers are being considered [23–25]. For the M4–M7 instruments, an option is to develop a seven-pixel hexagonal array, which will allow spectra in seven positions to be obtained simultaneously and will speed up mapping.

A spectrometer based on streaming signal processing using the fast Fourier transform will be placed at the output of the receivers for reading intermediate frequency signals. To ensure high spectral resolution, the output spectrometer channel width will be no worse than 25 kHz, which will make it possible to analyze the profile details of even the narrowest spectral lines of the studied range.

To solve the planned tasks of studying protoplanetary disks and comets, it is necessary to register HDO lines at a level of 5–10 mK (see [26–28]). The typical brightness of the lines of the main isotopologue of water in protostellar cores, where the lines are weak, is about 20–100 mK (for example, [29]); in protostars of different masses, the brightness of the main isotopologue reaches 1000 mK or more. Thus, it is necessary to detect the lines of water and isotopologues in the ground and excited states at a level of 10–100 mK. One should also take into account the fact that, in the protoplanetary disks, the brightness of the water line at 1113 GHz is about 10–20 mK [30], and in protostars and comets, the brightness is about 100–1000 mK [12, 31].

The posed tasks require long-term signal accumulation (integration) for some types of objects, which becomes clear from the analysis of the fundamental relationship among the noise of the entire system (receiver + Earth + atmosphere + cosmic source), $T_{\rm sys}$; the spectral resolution, Δv; the integration time, τ; and the limiting standard deviation of the noise, ΔT [32]:

$$\Delta T = \frac{T_{\rm sys}}{\sqrt{\Delta v \tau}} \,. \tag{1}$$

Since atmospheric noise can be ignored in the orbit of the Millimetron Space Observatory, and the relatively narrow main lobe of the telescope beam pattern Θ (see Table 1) allows one to rule out the noise from Earth, the values of $T_{\rm n}$ can be used as $T_{\rm sys}$ to estimate the integration time upon reaching the required sensitivity.

Using formula (1) and the results of water line observations from the Herschel telescope, one can estimate the integration time for observing various types of objects. It should be borne in mind that the desired noise level ΔT should be 5–10 times lower than the source brightness, also expressed in temperature units according to the Rayleigh–Jeans law. For example, to observe low-mass protostars in the ortho-H_2O $1_{1.0}$–$1_{0.1}$ line at a frequency of 556.9 GHz, a sensitivity of 10 mK is required, and a spectral resolution of 0.3 km s^{-1} (Δv of about 557 kHz) is sufficient to detect the line [33]. Note that the spectral resolution is usually higher when studying the structure and kinematics of objects. At the Millimetron Space Observatory, this level will be achieved within 12 min of integration. Prestellar cores require greater sensitivity, up to 2 mK [29], which leads to 4.9 h of integration in the direction of the object. For protoplanetary disks [30] and comets [26], the observation time needed to detect water lines and their isotopologues also takes several hours of integration for each of the objects. It should be emphasized that the costs of actual observation time can be up to 2.5 times higher due to the need to observe the sky background, to calibrate and point the telescope at the object, and to adjust the frequency.

3. Formation of water in interstellar medium

The formation of water molecules in the interstellar medium and molecular clouds is a small part of a larger scheme that includes several hundred components, thousands of gas-phase chemical reactions (see, for example, [34, 35]), and processes on the surface of dust particles [36]. How the water molecules are formed in the ISM is among the most studied pathways of chemical transformation of matter in space. A detailed reaction scheme of water molecule formation in the ISM is shown, for example, in Fig. 16 from [37]. In the gas phase at low temperatures, the 'cold' ion-molecular pathway of water molecule formation dominates through a sequence of reactions:

- $O + H_3^+ \rightarrow OH^+ + H_2$,
- $OH^+ + H_2 \rightarrow H_2O^+ + H$,
- $H_2O^+ + H_2 \rightarrow H_3O^+ + H$,
- $H_3O^+ + e^- \rightarrow H_2O + H$.

The appearance of the H_3^+ ion initiating this chain is associated with the ionization of molecular hydrogen by cosmic ray particles [38].

At gas temperatures above 250 K, the contribution of the 'hot' pathway of water molecule formation increases, initiated by the endothermic reaction

- $+ H_2 \rightarrow OH + H$,

followed by the reaction

- $OH + H_2 \rightarrow H_2O + H$.

These reactions actively proceed in the vicinity of protostars with temperatures above several hundred kelvins and in the

regions of propagation of shock waves (SWs), behind the fronts of which the gas is heated to several thousand kelvins.

However, the described gas-phase channels of water formation cannot explain the amount of water observed in dark molecular clouds and prestellar cores [36, 39, 40]. To explain the observed water content in such objects, reactions of water formation on the surface of interstellar dust are used [41]. For a long time, the classical low-temperature pathway of water ice formation on the surface of dust was considered to be the sequential hydrogenation of oxygen atoms by hydrogen atoms with the intermediate formation of hydroxyl according to reactions

- $O + H \rightarrow OH$,
- $OH + H \rightarrow H_2O$,

considered in [41–43]. The exothermic nature and the absence of an activation barrier in the reactions of association between atoms and free radicals contribute to the efficient occurrence of these reactions at temperatures on the order of 10 K. A dust particle is a third body that allows excess energy to be dissipated from these reactions, which is impossible in the gas phase at pressures characteristic of the early stages of star formation.

The conventional division of the main channels of water formation into thermal phases can correspond, for example, to the different thickness of the gas layer near young stars, where ultraviolet (UV) photons penetrate the interstellar medium, ionizing and heating it [44–46]. To characterize the depth of photon penetration into matter, astrophysics usually uses the value of A_V — absorption in the photometric band V, namely, near a wavelength of 5500 Å, measured in stellar magnitudes. It is important to note that interstellar medium is ionized not only due to UV photons emitted by young stars. In the dark regions of interstellar clouds, where the absorption of external photons reaches values of $A_V \sim 3-8^m$ (m is the stellar magnitude), the main ionization agents are cosmic rays, which penetrate molecular clouds with high efficiency to a considerable depth ($A_V > 10^m$ (see [47])). Thus, even in the inner regions of clouds that are well shielded from external UV radiation, nonzero concentrations of molecular ions are maintained, which ensures the efficient occurrence of ion-molecular reactions leading to the formation of such precursor molecules of gas-phase water as OH^+, H_2O^+, and H_3O^+, in accordance with the above-mentioned 'cold' scenario. However, it must be remembered that, at the low temperatures characteristic of the dark regions of molecular clouds, water molecules formed in the gas phase gradually freeze on dust particles.

The destruction of water molecules in collisions with hydrogen atoms,

- $H_2O + H \rightarrow OH + H_2$,

in dense molecular clouds is unlikely due to both the low concentration of atomic hydrogen and the high temperature ($T \gtrsim 10^4$ K) required for this reaction to occur. Therefore, the destruction of water molecules in the gas phase occurs mainly due to photodissociation by UV quanta with a wavelength of 983–1800 Å. X-ray radiation also leads to the destruction of water molecules in ion-molecular reactions due to an increase in the content of molecular ions HCO^+, H_3^+, H^+, He^+, as well as photodissociation of water [48–50].

Subsequently, alternative reaction pathways for the formation of water on the surfaces of dust particles with the participation of molecular hydrogen were proposed [51–53]. In particular, Oba et al. [51] demonstrated in laboratory conditions that water ice can form on the surface at a temperature of 10 K in the exothermic reaction

- $OH + H_2 \rightarrow H_2O + H$,

and its significant activation barrier (2100 K [54]) is overcome by quantum tunneling of the hydrogen atom. Despite the lower rate of this reaction compared to the classical reaction $OH + H \rightarrow H_2O$, an argument in favor of the reaction path proposed in [51] is the high concentration of molecular hydrogen both in the gas phase and on the dust surface.

Lamberts et al. [52] considered the possibility of water ice formation at temperatures of 10–20 K in the reaction $O + H_2 \rightarrow OH + H$ both in laboratory conditions and using kinetic Monte Carlo simulations. In contrast to the interaction of hydrogen molecules with hydroxyl, studied in [51], the endothermic nature of the interaction of oxygen atoms with hydrogen molecules limits the efficiency of this reaction on the dust surface at low temperatures. Nevertheless, Lamberts et al. [52] obtained an upper limit on the contribution of the reaction $O + H_2 \rightarrow OH + H$ to the formation of water ice, equal to 11%.

Although the pathways for the formation of water ice involving hydrogen molecules were proposed more than 10 years ago, most modern astrochemical models take into account the classical ways for the formation of water ice involving hydrogen atoms. This is partly due to the computational costs of including hydrogen molecules in astrochemical models [55, 56]. Thus, the exact pathway for the formation of water ice on the dust surface remains controversial.

One of the possible indicators of a specific scenario for the formation of water ice (with the participation of hydrogen atoms or molecules) is the observed ratios of isotopologues $H_2O/HDO/D_2O$. Deuterium fractionation due to reactions on dust [57, 58] and in the gas phase (for example, [59, 60]) leads to an increase in the abundance of OD, HDO, and D_2O molecules. Due to deuterium fractionation (for example, [61, 62]), the ratios of HDO/H_2O and D_2O/H_2O abundances are significantly higher than the D/H ratio of $\sim 2 \times 10^{-5}$, determined for the local interstellar medium [63].

Several factors are responsible for an increase in the abundance of deuterium on dust. First, the gas is enriched in atomic deuterium due to the preferential formation of D as a result of the recombination of H_2D^+ with an electron [12]. In the gas phase, molecules of semi-heavy and heavy deuterated water HDO and D_2O are formed in the same processes as the formation of light water. Second, it is important for reactions on the dust surface that D atoms be heavier, and so, when colliding with the dust surface, the probability of an elastic collision (rebound) is less than that of H. Consequently, further fractionation occurs, which leads to an overall increase in the abundance of D compared to the that of H. Third, D atoms are heavier than H atoms and have a higher adhesion energy on the dust surface. Thus, deuterium, on average, lives longer on the dust surface and desorbs less often, further facilitating fractionation. In general, all of the listed factors should lead to an overall enrichment of chemical compounds on the dust surface with deuterium compared to the elemental D/H ratio.

The reactions of association of hydrogen atoms with oxygen atoms and hydroxyl radicals (the main chain of reactions) do not have a pronounced isotope effect. In this case, the H/D ratio in the resulting water molecules should be determined by the ratio of H and D atoms on the dust surface and their diffusion rates (see Fig. 5 from [12]). However, there are features of the reactions on dust inherent in the chemical

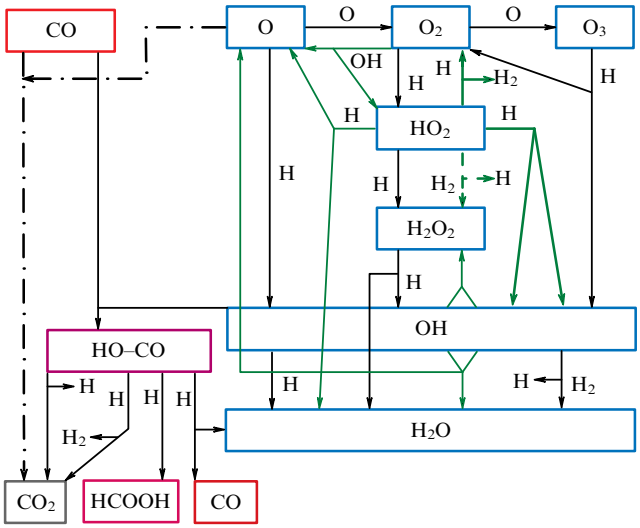

Figure 1. Black arrows between blue rectangles show main stages of water ice formation on dust surface from oxygen atoms. Green arrows demonstrate secondary pathways known after experiments [68]. For clarity, main competitive pathways for consumption of oxygen atoms and hydroxyl radicals leading to formation of CO_2 ice are also shown. Figure is adapted from [69].

chains of water formation which can reduce the final HDO/H_2O ratio on dust. Oba et al. [51] point to a significant isotope effect in the case of water molecule formation through quantum tunneling with the participation of hydrogen molecules in the reaction $H_2 + OH \rightarrow H_2O + H$. The tunneling rate of hydrogen atoms is several times higher than that of deuterium atoms, and so the rates of the $HD/D_2 + OH$ reactions will be an order of magnitude slower. In this case, the formed water molecules should be depleted in deuterium, as opposed to other hydrides formed by interaction with hydrogen atoms on the dust surface, such as NH_3 and possibly CH_4 [64], since the reactions of formation via H_2/HD proceed without a barrier for the latter two molecules.

Observation of the 'cold' H_2O and HDO lines is one of the main tasks of the Millimetron Space Observatory. Determining the isotopic ratios in water molecules in the direction of different star-forming regions will bring us closer to establishing the exact pathways of water ice formation.

Following recent observations of molecular oxygen in the comas of comets 67P/Churyumov–Gerasimenko and 1P/Halley with O_2/H_2O ratios of $3.1 \pm 1.1\%$ and $3.7 \pm 1.7\%$, the discussion of the role of molecular oxygen in the formation of water ice has been renewed. The channels of water formation involving O_2 were studied in detail in [36, 65–68] using a combination of laboratory and numerical methods. The most complete network of reactions of water molecule formation on the surface of interstellar dust is presented in Fig. 1.

Already at the stage of translucent and dark molecular clouds, the main mass of water is concentrated in the solid phase. The energy of desorption of water molecules from the surface of water ice in temperature terms is ≈ 5800 K [70, 71]. Low temperatures characteristic of translucent and dark clouds make the mechanism of thermal desorption ineffective. It is assumed that nonthermal mechanisms are responsible for the transfer of water molecules from the dust surface to the gas phase, with the main one being considered to be that of desorption induced by the absorption of a UV photon (photodesorption, see [72–75]). Of the alternative (parallel) mechanisms, the main focus is on that of desorption of a water molecule due to excess energy from the reaction of its formation ('reactive desorption' [76]), as well as the partial loss of the ice mantle as a result of the interaction of a dust particle with cosmic rays [77–79].

In the case of the reactive desorption mechanism, establishing the exact pathway of formation of water molecules on the dust surface directly affects the probability of transfer of these molecules into the gas phase. In the reaction $OH + H_2 \rightarrow H_2O + H$, the excess reaction energy is distributed between the two reaction products and the dust particle, whereas in the reaction $OH + H \rightarrow H_2O$, the excess energy of water formation is distributed between the dust particle and the only reaction product. In the latter case, a higher probability of transfer of the molecule into the gas phase should be expected. A direct influence on the ratio of isotopologues HDO/H_2O in the gas phase can also be expected. The isotope effect of the reaction $OH + H_2 \rightarrow H_2O + H$ will predominantly enrich the gas phase with water molecules depleted in deuterium compared to the ratio between hydrogen and deuterium atoms in the gas phase.

Indirect information about the main contribution of one of the above-mentioned nonthermal mechanisms of water transfer from the dust surface to the gas can be obtained by measuring the temperature of water molecules in the gas phase and the ratio of the ortho- and para-spin isomers of water molecules. Indeed, the deviation of the ratio of the ortho- and para-spin isomers of water observed in cometary comas from the equilibrium ratio of 3 was used as one of the arguments in favor of water formation on the dust surface at low temperatures [80, 81]. However, laboratory measurements of this ratio for water molecules in the gas phase obtained by photodesorption (one of the possible mechanisms of nonthermal transfer of water molecules to the gas phase) yielded a value equal to that of equilibrium [82, 83]. In turn, van Dishoeck et al. in their review [12] point out the absence of indisputable observations of a deviation of the ratio of the ortho- and para-spin isomers of water from a value of 3 in observations of molecular clouds, which leaves the issue debatable. Measurements of the ratio of ortho- and para-spin isomers of water in the direction of various star-forming regions are among the main tasks of the Millimetron Space Observatory.

Note that solving the problem of water desorption from ice mantles is important not only from the point of view of water evolution. Experiments (for example, [84]) show that, when water-rich ice evaporates, other molecules enter the gas phase along with water molecules, regardless of their desorption energy.

For a long time, the proposed theoretical pathways for the formation of water ice on the surface of dust had no direct experimental confirmation. Technical progress in the development of ultra-high vacuum and cryogenic equipment has opened up the possibility of fabricating specialized instruments for the detailed experimental study of surface phenomena occurring during the accretion of hydrogen and oxygen atoms and molecules from the gas phase onto various surfaces cooled to a temperature of 10–15 K. The core of such instruments is an ultra-high vacuum chamber in which a pressure of up to 10^{-13} atm is produced using turbomolecular pumps [43, 65, 85–87]. A substrate continuously cooled by a

closed-loop helium cryostat is placed in the center of the ultra-high vacuum chamber. Oxygen and hydrogen atoms are generated by decomposition of various molecules in a non-equilibrium low-pressure plasma [43, 65, 85] or by passing the molecules through a hot tungsten capillary [86]. In both cases, atoms are generated in independent chambers, and mixed atomic and molecular beams are formed by using differential gas pumping systems, vacuum shutters, and guiding capillaries. Changing the substrate temperature, gas pressure, and plasma parameters or the temperature of the tungsten capillary allows the experimental parameters leading to the formation of water molecules on the substrate surface to be controlled. Thus, the first experimental confirmations of the formation of water ice were obtained under physicochemical conditions simulating those in the ISM. The use of infrared grazing incidence reflection spectroscopy made it possible to continuously monitor the ice composition and to study the kinetics of individual processes involved in the formation of water molecules on the dust surface [36, 68, 86].

4. Tasks for Millimetron Space Observatory

The problem of water origin requires a thorough verification of the theoretical concepts described in the previous section and the adaptation of the results of astrochemical experiments to space conditions. At present, the main challenges are related to the lack of understanding of the following questions.

• Is water contained in the composition of ice mantles of dust particles the main molecular reservoir of oxygen? What is the contribution of gas-phase pathways of water synthesis in space objects and what is the contribution of surface chemistry?

• If the answer to the first question is positive, then due to what process does water end up in the gas phase? This question requires an assessment of the efficiency of various mechanisms of desorption from dust to gas.

• Does the presence of water on dust particles affect the process of desorption of other molecules? Do molecules, including complex organics, fly out of the mantles together with water? This question is important not only for understanding the synthesis of water, but also for understanding its transfer, as well as the transport of complex organic molecules.

• What features of the formation and propagation of shock waves in the ISM lead to an increase in the water content in the gas phase? Which regions near the shock front are traced by water emission lines?

These questions are discussed in detail in Sections 4.1–4.3.

To establish the connection between the chemical composition of molecular clouds, protoplanetary disks, comets, and the origin of life on Earth, it is necessary to understand how water is transferred among these objects. A detailed discussion is given in Section 4.4. The key questions here are the following.

• What is the role of comets in the origin of Earth's water?

• Do comets inherit water (or the entire chemical composition) from the peripheral regions of protoplanetary disks?

As part of the Millimetron Space Observatory's program to study the origin and transfer of water in the Universe, it is planned to observe a number of the most important spectral lines of water, which will help answer the above questions. Detecting a larger number of water lines will provide more information about the physical state of the molecular gas and the water content in it. To limit the range of physical parameters, additional observations of the lines of atoms, ions, and molecules that are indicators of physical conditions in the medium, such as CII, OI, H_2D^+ SiO, H_2CO, and CH_3OH, are provided. To study the contribution of gas-phase chemistry to water synthesis, observations of intermediate components of chemical chains of water formation are planned, in particular, OH and molecular ions OH^+, H_2O^+, H_3O^+. The frequencies of some selected transitions are listed in Table 2.

Table 2. Some oxygen-containing molecules and transitions * available for observations with Millimetron Space Observatory.

Molecule	Transition	Frequency, GHz
CO	5–4	576.3
CO	7–6	806.7
CO	10–9	1151.9
CO	12–11	1381.9
OH	$^2\Pi_{3/2}$ $J = 17/2$, $F = 8-9$	1159.7
OH	$^2\Pi_{3/2}$ $J = 17/2$, $F = 8-9$	1321.8
OH	$^2\Pi_{3/2}$ $J = 9/2$, $F = 4-5$	1899.6
H_3O^+	$4_{1.0} - 3_{1.1}$	1092.5
H_3O^+	$8_{4.1} - 8_{4.0}$	1387.8
SiO	12–11	520.9
SiO	13–12	564.2
SiO	18–17	780.9
SiO	19–18	824.2
SiO	25–24	1083.7
SiO	26–25	1126.9
SiO	27–26	1170.1
SiO	28–27	1213.2
SiO	31–30	1342.6
SiO	32–31	1385.7
CH_3OH	$9_{3.7} - 9_{2.8}$	529.9
CH_3OH	$7_{3.5} - 6_{2.4}$	590.3
CH_3OH	$6_{4.3} - 5_{3.2}$	815.1
H_2CO	$8_{1.8} - 7_{1.7}$	561.9
H_2CO	$11_{1.11} - 10_{1.10}$	770.9
H_2CO	$11_{1.10} - 10_{1.9}$	823.1
H_2CO	$16_{1.15} - 15_{1.14}$	1188.0
H_2CO	$18_{1.17} - 17_{1.16}$	1330.8
H_2D^+	$2_{1.1} - 2_{1.2}$	1111.5
H_2D^+	$1_{0.1} - 0_{0.0}$	1370.1

* Only some of the most intense transitions of oxygen-containing molecules are given as an example. In total, hundreds of transitions of molecules such as OH, OH^-, H_3O^+, H_2O^+, H_2CO, CH_3OH, SiO, and CO fall within the range available for observations with the Millimetron Space Observatory. H_2D^+ molecule is also added, since it is important for studying early stages of formation of protoplanetary disks.

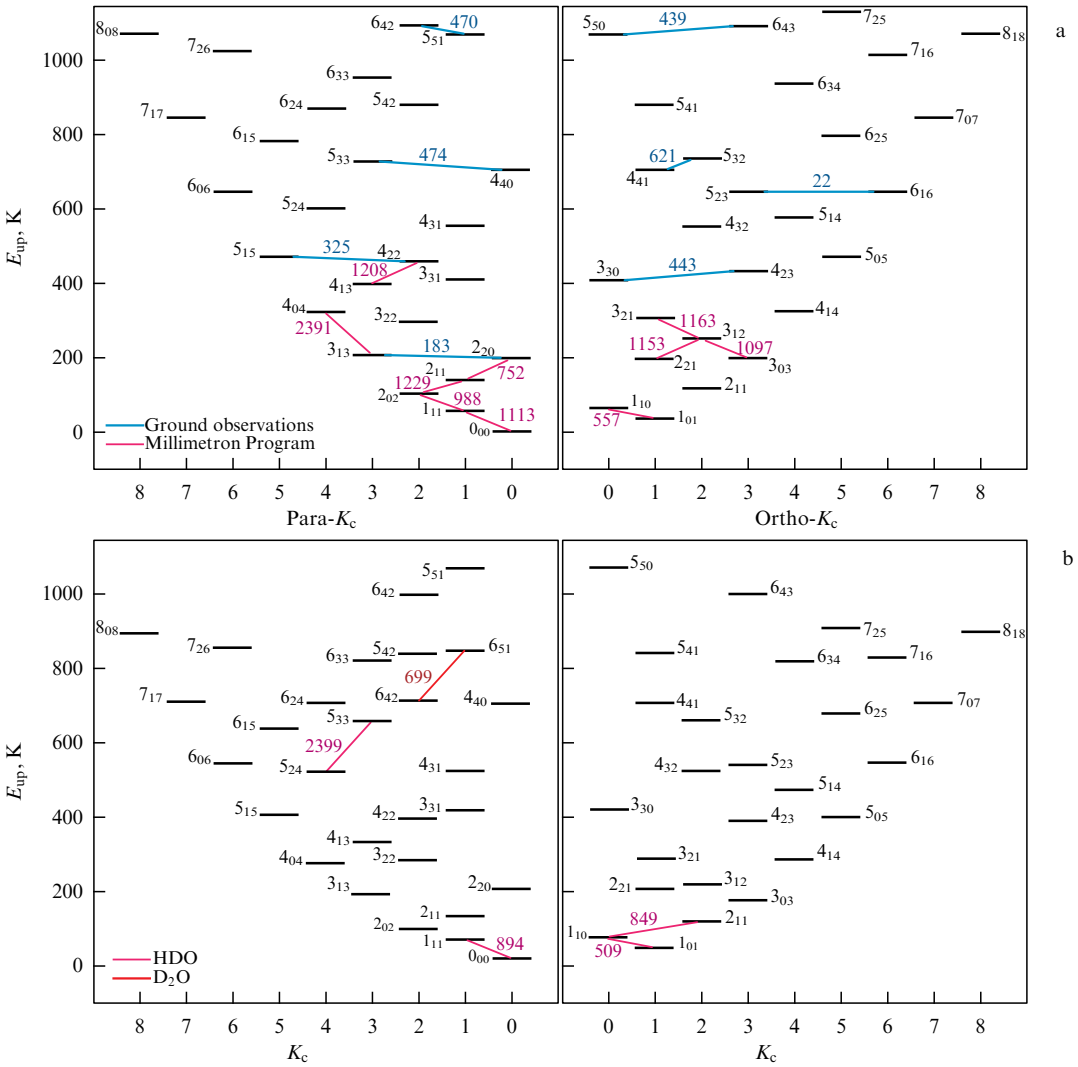

Figure 2. (a) Diagram of levels of ortho- and para-H_2O and transitions that are in the frequency range of Millimetron Space Observatory (indicated by pink lines). Transitions in H_2O molecule visible from Earth's surface are shown in blue (they are mainly observed as maser ones). (b) Diagram of levels for HDO molecule and transitions that are in the frequency range of Millimetron Space Observatory. Transition in D_2O molecule is shown by red line. Excitation levels of water molecules are characterized by three quantum numbers: J, K_a, K_c, where J is angular momentum, and K_a and K_c are projections of angular momentum onto molecular axis. K_a axis is bisector of H–O–H angle, and K_c axis lies in plane of the molecule and is perpendicular to K_a.

Transitions in a water molecule can be divided into three groups (Fig. 2): 'cold' water includes transitions with an excitation temperature of up to 200 K; 'warm' water, up to 500 K; and 'hot' water, up to 900 K, according to the gradation from paper [88]. Most of the 'cold' water lines fall in the ranges of 500–600 and 1000–1200 GHz, which are not accessible to ground-based instruments; some fall in the intermediate range of 740–900 GHz, part of which can be studied from Earth's surface. Higher transitions of 'warm' and 'hot' water can only be detected by orbital telescopes: the transition frequencies lie in a significantly higher-frequency region of the spectrum, up to 4–5 THz.

4.1 Water in molecular clouds and problem of oxygen deficiency

Studies of the formation of water molecules in the Universe are closely related to the problem of oxygen deficiency, a current description of which can be found in [12]. Here, we will give a brief summary of this problem, supplementing it with information from recent studies. Measurements of the oxygen content relative to hydrogen nuclei in the solar atmosphere give a value of 4.9×10^{-4} [89], while measurements of the content in main-sequence B stars in the solar neighborhood give a higher value of 5.8×10^{-4} [90]. Measurements of the gas-phase oxygen content in the ISM have shown that its average content relative to hydrogen nuclei is $N(O)/N(H) = 3.2 \times 10^{-4}$, which is 1.5–1.8 times less than the content in stars in the solar neighborhood, while the accuracy of determining the content is about 20% [91].

If the above-described theoretical concepts of water synthesis in the ISM are correct, and the data from laboratory measurements are correctly transferred to physical conditions in space, then this is the maximum oxygen content that can be contained in the mantles of dust particles. About 20% of the oxygen is apparently contained in the refractory cores of dust particles [92]. Summing up the gas-phase content in diffuse clouds and the assumed content in refractory cores, it is not possible to obtain a value equal to that observed in B stars. Several different versions have been proposed to explain the oxygen deficiency in the solar

neighborhood: enrichment of the matter of the Early Solar System with oxygen due to the outburst of a nearby supernova; fallout of metal-poor matter from dwarf galaxies in the solar neighborhood; migration of the Sun to the periphery of the Galaxy, where the metallicity is lower; and, finally, the assumption that oxygen is located in refractory matter that has not yet been identified [92].

To estimate the maximum possible water content that can be contained in the mantles of dust particles, it is necessary to remember that some amount of oxygen is contained in CO molecules. Taking into account the results of measuring the elemental content of carbon in the diffuse medium $N(\mathrm{CO})/N(\mathrm{H}) = (1.3-1.6)\times 10^{-4}$ [93, 94] and the content of CO molecules in the diffuse medium $N(\mathrm{CO})/N(\mathrm{H}) < 2\times 10^{-4}$ [95], the water content on dust relative to hydrogen nuclei can be estimated to be at a level of 2×10^{-4} or $N(\mathrm{H_2O})/N(\mathrm{H_2}) \approx 4\times 10^{-4}$.

However, infrared (IR) spectroscopy shows that the content is $N(\mathrm{H_2O})/N(\mathrm{H_2}) \ll 4\times 10^{-4}$ and not all oxygen is contained in water molecules in the mantles of dust particles. For example, based on measurements with the Spitzer and Herschel telescopes, Gibb et al. [96] and Oberg et al. [97], respectively, found that $N(\mathrm{H_2O})/N(\mathrm{H_2}) \approx 5\times 10^{-5}$ in the directions of star-forming regions. Recent measurements with the JWST telescope in star-forming regions show somewhat larger values of $(6-8)\times 10^{-5}$ (see [40]), which is still much less than the potential value. Therefore, not all gas-phase oxygen that could potentially be present in the composition of icy mantles is present in them. One possible explanation for the lack of water in the mantles is its desorption or destruction under the action of UV and/or X-rays/cosmic rays and the transition of oxygen into other compounds. In addition to studying desorption mechanisms and comparing their efficiency under different physical conditions, it is necessary to have estimates of the content of oxygen-containing molecules in the same objects where there are data on the water content. Some oxygen may be in the atomic state, but large samples of water, OI, and other oxygen compounds in the same objects are currently absent. Observations with the Millimetron Space Observatory will fill this gap. Below, we consider in detail the estimates of the water content in objects of different types.

4.1.1 Water in regions of interaction of supernova remnants with molecular clouds. Theoretical models of the formation of water molecules in the interaction of supernova remnants with molecular clouds show that water in these environments should be the dominant coolant of interstellar gas [98, 99]. However, observations do not confirm this. For example, Rho et al. [100] showed that the water content in the interaction region of the supernova remnant G349.7 + 0.2 is $\mathrm{H_2O/H_2} \approx 10^{-7}-10^{-6}$. Consequently, not all oxygen — only 0.1–1% of its content — is bound in water molecules. Perhaps the problem with the analysis of observations lies in the fact that use was made of the H_2O lines and the diagnostic CO and OH lines measured by different instruments with different spatial and spectral resolutions. The Millimetron Space Observatory, which will have a much higher spatial resolution, is capable of resolving compact regions of interaction of supernova shock waves with clumpy molecular clouds at ~ 0.3 pc [101]. In addition, near supernova remnants, water can be destroyed by X-ray and gamma radiation in C-type shock waves [102, 103], which leads to an increase in the $\mathrm{OH/H_2O}$ abundance ratio.

4.1.2 Water in diffuse molecular clouds. In diffuse molecular clouds, a rich molecular composition due to low reaction rates and a destructive effect of UV radiation on molecules should not be expected. Diatomic molecules are widely observed in the diffuse medium: H_2 [104, 105], CO [106], C_2 [107], and many hydrides [108]. Astrochemical simulation of the synthesis of molecules in interstellar clouds shows that water formed on the dust surface and desorbed into the gas phase should be present in a diffuse medium and have a relative content of $x_{\mathrm{H_2O}} \leqslant 10^{-8}$ [12, 109]. However, repeated attempts to detect water in diffuse clouds have been unsuccessful. Thus, Snow [110] reported an attempt to detect water absorption lines at a wavelength of $\lambda \approx 1240$ Å in the direction of ζ Ophiuchi with the Copernicus telescope. Snow [110] failed to detect these lines, but found OH and CO_2 lines, which are alternative oxygen reservoirs to water. Spaans et al. [111] also made an attempt to find water in a diffuse medium with the HST telescope in the direction of the star HD 154368 at the same wavelength. The attempt was unsuccessful and only the upper limit of $N(\mathrm{H_2O}) \leqslant 9\times 10^{12}$ cm^{-2} was estimated.

Water was first discovered in diffuse clouds using observations with the Submillimeter Wave Astronomy Satellite (SWAS) (see paper [112]). The ortho-H_2O absorption line at $\nu \approx 557$ GHz was detected toward the bright sub-mm source W51, with the line of sight piercing several spiral arms of the Galaxy during observations. The estimate of $N(\mathrm{H_2O}) = 2.5\times 10^{13}$ cm^{-2} is approximately three times greater than the values in the directions of the nearest diffuse clouds, which were studied using UV absorption lines. In addition, Neufeld et al. [112] measured a concentration ratio of $\mathrm{OH/H_2O} = 3$, which exceeds the ratio characteristic of low-temperature ion-molecular reaction chains. The high $\mathrm{OH/H_2O}$ ratio and the fact that the value of $N_{\mathrm{H_2O}}$ turned out to be several times greater led the authors to the idea that toward W51 there are several diffuse clouds and, in addition, there is a warm molecular gas in which water is actively formed in high-temperature neutral-neutral reactions.

Subsequent observations with the Herschel telescope led to the conclusion that water in diffuse clouds can have different origins. Thus, Flagey et al. [113] performed observations of the diffuse medium in spiral arms toward six regions of the formation of massive stars from different spiral arms of the Galaxy, observing not only ground state transitions but also excited state transitions of ortho-H_2O and para-H_2O, as well as ground state transitions of the H_2^{18} isotopologue. They found that $N(\mathrm{H_2O})$ in the diffuse medium lies in a wide range, from 10^{12} to 10^{14} cm^{-2}, with a content of relatively molecular hydrogen of $X_{\mathrm{H_2O}} \sim 5\times 10^{-8}$ and a content of relatively atomic hydrogen of $x_{\mathrm{H_2O}} \sim 10^{-8}$. Flagey et al. [113] did not find absorption lines corresponding to transitions between excited states; using this fact, they estimated that at least 85% of water molecules in diffuse clouds are in the ground state. For most of the observed objects, the ortho-H_2O/para-H_2O ratio of 3 was determined, but for several objects it was < 2.5, which is apparently due to the fact that, in this direction, water in the Galaxy is formed in cold gas or on cold dust. Thus, the study of the ortho-H_2O/para-H_2O ratio in diffuse clouds is interesting from the point of view of the history of the formation of molecular clouds and ice mantles in clouds. Flagey et al. [113] showed that, of all the observed water lines, only the one at 752 GHz is not distorted by the self-absorption effect; therefore, to study a diffuse medium, it is desirable to use this line in combination with transitions to the ground state.

4.1.3 Water in cores of molecular clouds and protostellar envelopes. *Prestellar cores within molecular clouds.* Individual stars and low-multiplicity systems are formed in dense prestellar cores within molecular clouds, and the physical conditions in them are directly related to the properties of future protostars, protoplanetary disks, and, finally, new planets. Several decades of continuous observations of these objects in molecular lines and the dust continuum made it possible to reconstruct their structure at scales of $\sim 10^4$ AU, and after the launch of the ALMA interferometer, at smaller scales of $\sim 10^3$ AU (see, for example, [114]). The study of these objects is necessary for understanding the initial conditions of star formation, since the molecular composition of the star-forming region at this stage is possibly reflected in the composition of protoplanetary disks.

Water is the most important reservoir of oxygen in the prestellar cores of molecular clouds. Numerous models of the chemical evolution of these objects show that oxygen should be mainly concentrated in the icy mantles of dust particles (for example, [115]). Caselli et al. [29] reported observations of the ortho-H_2O $1_{1.0} - 1_{0.1}$ line in the protostellar core of L1544. They were able to estimate $N(H_2O) > 1.0 \times 10^{13}$ cm^{-2}, corresponding to the gas-phase water content of $N(H_2O)/N(H_2) \geqslant 1.4 \times 10^{-10}$, which is 10^5 times lower than its content in the icy mantles of dust particles (see, for example, [40]). Caselli et al. [29] concluded that water is formed in this object during reactions on the surfaces of dust particles and that the water content in the gas phase is maintained due to photodesorption of water from the mantles of dust particles by cosmic-ray-induced photons. However, somewhat later than the publication of [29], a new mechanism of desorption from dust was proposed — reactive desorption (see, for example, [55]), whose efficiency is higher, which means that there should be more water in the gas phase in the protostellar core. In general, it is not yet possible to explain the observed amount of water in the gas phase.

To date, Caselli et al. [29] are the only authors that have reported on the confident detection of a spectrally resolved line of water in the protostellar core. Unfortunately, no single map of water emission in objects of this type has been obtained yet. Having maps and, consequently, having constructed spatial distributions of water in protostellar cores, including ortho- and para-modifications, one can understand the adequacy of today's ideas about the chemical chains of water formation, in particular, about the mechanisms of desorption and the contribution of the gas-phase and surface channels of water synthesis.

The parameters of the Millimetron Space Observatory are optimally suited for observing water in protostellar cores. A spectral resolution of about 0.25 km s^{-1} and higher will allow spectral lines to be resolved, with high angular resolution making it possible to obtain water emission maps. Mapping HDO lines in protostellar cores and their molecular envelopes will help in understanding whether water at this stage of star formation is similar to that in comets and Earth's ocean.

In protostellar cores, water can also appear as absorption features against the background of a bright dust continuum, which provides additional information about the gas kinematics in objects and the distribution of gas-phase water in them. Figure 3 shows a synthetic spectral map in the ortho-H_2O $1_{1.0} - 1_{0.1}$ line for a model protostellar core in a molecular cloud, obtained using the code from [116, 117] and the radiative transfer model [118, 119]. One can see that the shape of the spectrum changes with increasing density,

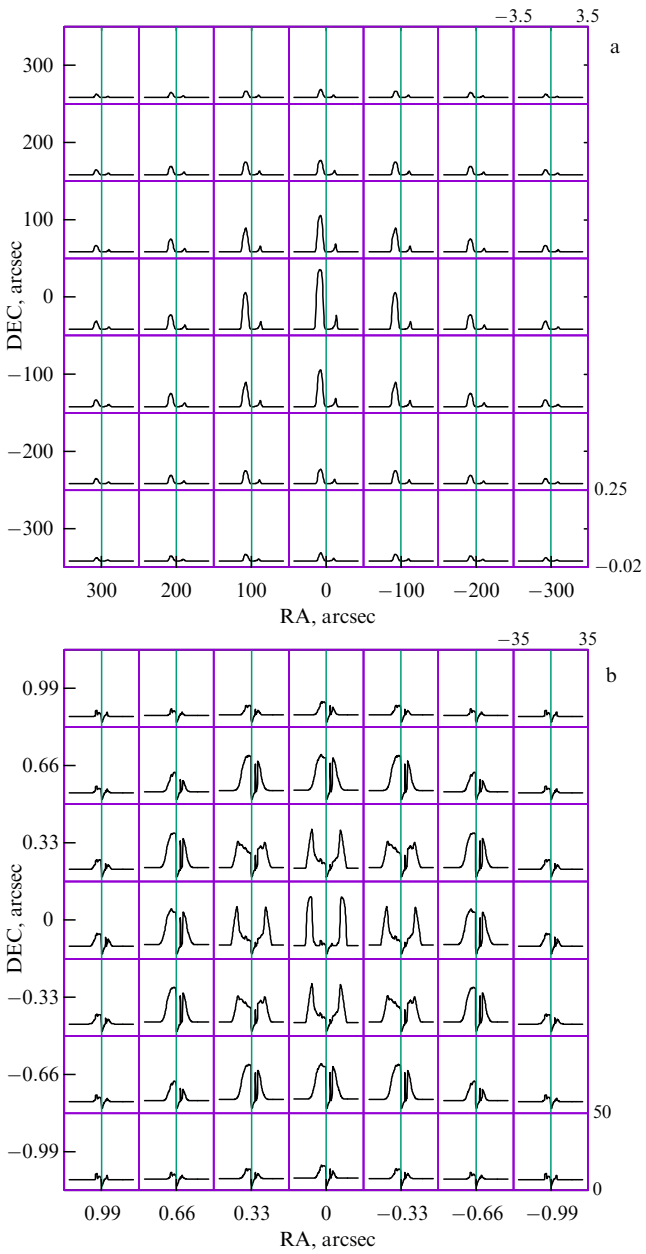

Figure 3. Synthetic maps of water lines at a frequency of 556.9 GHz for (a) a prestellar dense molecular cloud with signs of collapse and (b) with a protostar with a mass of 11 $M_\odot$ in the center. Brightness temperature along ordinate axis is expressed using Rayleigh–Jeans scale. Velocity along abscissa axis is measured in km s^{-1}. RA (right ascension) and DEC (declination) are celestial equatorial coordinates. Figure shows coordinate values relative to centers of maps.

which accompanies gravitational collapse and the formation of a protostar in the cloud. The P Cyg profile has two components: the blue one represents the dense gas in the central part of the prestellar core, and the red one is formed in the outer shell collapsing into a protostar. Figure 3a shows a map for a prestellar core.

Water in protostellar envelopes. Studying the shock-wave propagation regions in protostellar envelopes and the vicinity of young stars allows one to test theoretical and laboratory concepts of the chemical chains of water formation due to the relative proximity of these objects. A theoretical map of water line profiles near a massive protostar is shown in Fig. 3b. One can see that the brightness of the lines has increased by more

than an order of magnitude compared to prestellar cores, which means that such lines are easier to observe. Such studies can be aimed at solving the key issue of the lack of water in the icy mantles of cosmic dust particles. The more global problem of oxygen deficiency was mentioned above, but it also applies specifically to water: it is still unclear why not all the oxygen not bound to carbon in CO molecules, or at least not a large part of it, ends up in water in the icy mantles of dust particles. Observations of various water emission lines at different distances from the protostar will allow the contribution of desorption and gas-phase reaction chains to be assessed at different values of temperature, density, and composition of the ice mantles.

The low water content on dust can be explained by assuming that there is not enough time for all the oxygen to completely convert into these molecules and that the protostellar stage takes $\sim 10^5$ rather than $\sim 10^6$ years. As a result, much oxygen in the gas phase remains in atomic form and in the form of molecules of CO, CO_2, H_2CO, CH_3OH, etc. This issue is addressed in [115], where, using a dozen objects as examples, the agreement between the observed water content and the model of a short protostellar stage is demonstrated. Observations of other molecules in star-forming regions also support the idea of a short protostellar stage (see, for example, [120–122]), which is consistent with the paradigm of rapid star formation in the gravoturbulent model [123–125].

Another possible explanation for the low water content is related to the nonmonotonic nature of the accretion of the molecular cloud onto the protostar (see, for example, [126, 127] and also review [128]). This nature of accretion has been repeatedly confirmed by observations both in molecular lines and in the IR continuum (for example, [129]). Due to the episodic increase in the dust temperature during accretion bursts, part of the water mantle is desorbed from the dust surface, entering the gas phase, where it reacts with other molecules [130] (see also [131–133]). After the end of the accretion burst, the medium cools down only after some time; therefore, until the effective chains of reactions on the dust particles are resumed, water molecules are not formed. Then there is a new accretion burst, and so on.

The third option for explaining the low water content in protostellar envelopes is the assumption that observations of the absorption spectra of interstellar dust against the background of young stars yield an underestimated water content in the mantles, since the water is partially concentrated on the surface of large (1 μm or more) dust particles present even in dark prestellar clouds [134, 135]. They do not make a significant contribution to absorption in the mid-IR range and reduce the area of dust available for surface reactions. In addition, a fourth option is possible, in which oxygen is part of a hitherto unknown refractory substance.

The efficiency of the high-temperature channel of chemical reactions also raises questions, since the water content is also low in hot cores — envelopes of massive protostars, where complex organic molecules formed during surface reactions and desorbed into gas due to the high temperature of dust, $T_{\rm dust} > 100$ K, are actively observed. Observations show that $N(H_2O)/N(H_2) \lesssim 10^{-4}$, and more often it is in the range from 10^{-7} to 10^{-5} (see a detailed discussion of these results in review [12]). Only in a few hot cores does the content approach the elemental abundance of oxygen in order of magnitude (see [136]), and the authors suggested that not only thermal evaporation of mantles but also fragmentation of dust particles contribute to the appearance of water molecules in the gas phase. It is noteworthy that, despite the high temperature of the gas, the water content remains low, i.e., water is not effectively formed during neutral-neutral reactions. One explanation for the low water content may also be the dissociation of water after the molecules appear in the gas phase under the influence of high-power UV radiation from young stars (see, for example, [137]).

Upcoming observations with the Millimetron Space Observatory will help us to understand these issues. It will be possible to supplement the observations of transitions into the ground state in objects from the completed Herschel telescope programs with observations of higher transitions, as well as optically thin lines of water isotopologues, which will improve the accuracy of determining the content of gas-phase water and intermediate molecules from the chains of water formation in the shells of protostellar stars. Consequently, new constraints on the efficiency of gas-phase reaction chains will be obtained.

The regions near protostars and hot cores, where icy mantles are heated and evaporated, are very compact, with a typical angular size of $\lesssim 1''$ [138], and so observations with the Herschel telescope were burdened by serious radiation dilution, which made it difficult to analyze the data. A threefold increase in spatial resolution at the Millimetron Space Observatory will allow penetrating deeper into the thickness of protostellar envelopes and observing the immediate vicinity of protostars, where mantles evaporate.

It is clear that, to solve the problem of water deficiency in protostellar envelopes, detailed chemical dynamic simulation of protostellar envelopes and disks is needed, with the obligatory inclusion of episodic accretion in the model, which will allow future observations with the Millimetron Space Observatory to be interpreted using a self-consistent approach. Note that a non-LTE (local thermodynamic equilibrium) approach is needed to analyze the water emission lines, taking into account the lines of both low and high excitations [139–141].

If the Millimetron Space Observatory is able to detect radiation at shorter wavelengths, namely, observe the atomic oxygen [OI] lines at 63 and 145 μm, we will be able to determine the atomic oxygen content in the envelopes of protostellar objects with an unprecedentedly high spatial resolution. Consequently, it will be possible to answer the question of whether oxygen is contained in the atomic state in all objects of this type. Neither the Herschel telescope nor the SOFIA telescope has performed systematic observations in these two lines in the direction of hot cores and envelopes of low-mass protostars. To determine the oxygen content, two lines are needed, since the 63-μm line is usually optically thick [142–145]. In the near future, only the Millimetron Space Observatory will be able to solve the problem of oxygen deficiency and the related problem of water deficiency in the envelopes of protostellar objects.

4.2 Water behind shock-wave fronts

Shock waves occur in protostellar and young stellar objects, molecular clouds and filaments, star-forming regions, and outflows from active galactic nuclei. It is known that the emission in molecular lines reflects the physical state of the gas behind the shock-wave fronts [146, 147], and water molecules are one of the important indicators of the physical conditions in the medium [148, 149]. The presence of dust in the gas significantly affects the emission of water

molecules behind the shock-wave fronts [150]. Due to the inertia of dust particles, the structure of the shock wave changes depending on the gas density and the magnetic field strength. Thus, in addition to the classical *C*- and *J*-type shocks [151], there are also intermediate variants [152]. The dynamics of gas and dust under these conditions determine the chemical and thermal evolution of the gas behind the front and, therefore, the emission properties of water molecules [150, 153]. At shock-wave velocities above 50 km s^{-1}, molecules of H_2, H_2O, CO, etc., are destroyed as a result of collisional dissociation. Behind shock-wave fronts with a lower velocity, water molecules are effectively formed due to neutral-neutral reactions (see the description of reaction chains in Section 4.1). A wave velocity of higher than 15 km s^{-1} is sufficient to heat the gas behind the shock-wave front to 400 K and quickly convert oxygen atoms into water molecules. In cold molecular clouds, oxygen is not in the gas phase but is probably contained in the mantles of dust particles; therefore, the lower limit of the shock-wave velocity is different. To increase the fraction of oxygen in the gas phase, it is first necessary to destroy (evaporate) the mantles of the particles, which strongly depends on the shock-wave velocity: at a particle size of 0.3 μm, up to 10% and almost 100% of oxygen is released for velocities of 20 and 25 km s^{-1}, respectively [147]. Flower and Pineau des Forêts [154] showed that a velocity 2–2.5 times lower, about 10 km s^{-1}, is needed to destroy ice mantles. The higher velocity limit is associated with the peculiarities of the transition of oxygen from the particle mantles and the conversion of O and OH into water molecules [153, 155]. At a velocity of less than 10 km s^{-1}, water molecules can be formed in significant quantities only in dense fragments with a density of $n \gtrsim 10^4$ cm^{-3} under the action of a low UV radiation field comparable to the average interstellar field in the vicinity of the Sun (see [152]). The content of water molecules increases upon an increase in both shock-wave velocity and radiation flux. This is accompanied by an increase in the concentration of CO and OH molecules. Consequently, knowledge of the ratios of the beam concentrations of CO, OH, and other molecules will make it possible to limit the water content and determine the physical conditions in the medium behind the shock-wave fronts [150, 152].

4.2.1 Water emission lines as markers of shock waves in star-forming regions. The emergence of bright water emission lines accompanies the process of shock-wave propagation in the vicinity of young stellar objects, and the lines outside regions with active star formation are weak due to the low water content in the gas phase. Consequently, bright emission in water lines is an extremely informative marker of the star formation process. For individual lines, more than 60% of the integrated intensity of water emission lines results from cavities formed during the propagation of shock waves from young stars upon their formation [156]. The remaining energy emitted in the lines comes from the envelopes of young massive stars. Interestingly, the widths of quasi-thermal water lines in the regions of formation of massive and low-mass stars are approximately the same, which indicates the similarity of the outflows associated with shock waves in objects of two different types. In addition, San José-García et al. [156] showed for objects from our Galaxy that the luminosity in water lines is linearly proportional to the bolometric luminosity of the star-forming region.

The connection between water emission lines and star-forming regions is also confirmed by numerous observations of water vapor maser emission, since the conditions for the excitation of H_2O masers often arise during the interaction of shock waves, protostellar jets (bipolar flows) with the surrounding matter [157, 158]. Ladeyschikov et al. [4] studied the correlation between H_2O masers and infrared/submillimeter (IR/sub-mm) sources using data from two surveys: the Hi-GAL Galactic Plane Survey, conducted as part of the key Herschel Telescope program in five wavelength ranges from 70 to 500 μm [159], and the ATLASGAL survey, conducted on the APEX Telescope at a wavelength of 870 μm [160]. It was found that 88% of IR/sub-mm sources from the Hi-GAL and ATLASGAL catalogues are associated with H_2O masers. These IR/sub-mm sources are essentially clumps of matter inside molecular clouds and/or molecular filaments, i.e., these are places where stars are formed. Thus, H_2O masers are closely associated with star-forming regions and therefore, in one way or another, are markers of the star birth process.

4.2.2 Testing models of shock–wave propagation along water lines. Rich opportunities for water formation at high temperatures appear in the regions of interaction of supernova remnants with molecular clouds, which makes supernova remnants natural laboratories for studying the origin and transport of water. During the evolution before the supernova explosion, stars significantly change the circumstellar environment, blowing bubbles into the ISM with a nonstationary stellar wind [161, 162]. At the initial stage after the explosion, the supernova ejecta, enriched in metals, spreads along the complex multilayer structure of the bubble formed by the pre-supernova wind and its eruptive emissions before the explosion. Then, regardless of the size of the bubble before the explosion, the supernova ejecta and the circumstellar matter collected by it, called the 'supernova remnant,' go beyond the bubble and interact with the ISM. Since most supernova remnants are located in the plane of the Galaxy with a characteristic height above the galactic plane of $h \sim 50$ pc [163], many of them fly apart near or even inside molecular clouds. When a remnant interacts with dense clumps inside a molecular cloud, conditions are created for the formation of water in high-temperature reactions and its subsequent observation.

Emission lines of water were first detected in the supernova remnant 3C391 by the Infrared Space Observatory (ISO) with an excitation temperature within $T_{\rm upper} < 400$ K from the ground state [164].

The complexity of the problem of estimating the water content lies in a self-consistent description of the shock-wave propagation dynamics and solving a system of kinetic equations describing hundreds and thousands of gas-phase reactions. Moreover, gas clumps can be affected by not one but several shock waves. Observations of three spatially separated clumps in the supernova remnant IC443 in a common parent molecular cloud at the SWAS observatory in the ortho-H_2O $1_{1.0}$–$1_{0.1}$ line revealed a small ratio of $N(H_2O)/N(^{12}CO) = (2-5) \times 10^{-4}$, which contradicted the models of a single-shock interaction between the supernova remnant and a dense clump [165]. According to the hypothesis put forward in this paper, the observational data can be reproduced in a more complex model involving the action of a series (at least two) of successive shock waves on the clump.

Studying several regions of interaction between the shock wave of the supernova remnant and gas clumps, located at different distances both along the line of sight and from the center of the explosion, allows one to study the shock interaction of the supernova remnant with the gas in a wide range of mutual velocities and density distributions. Since the clumps belong to a common molecular cloud and have a common elemental composition, it is possible to track the dynamics of the interaction between the supernova remnant and the clumps and construct evolutionary tracks of the water content, comparing them with the results of numerical simulation. Thus, it becomes possible to trace in which places one channel of formation of water molecules or another predominates.

The spatial extent of the supernova remnants allows additional independent methods to be used for studying their physical properties and elemental and chemical composition of the surrounding ISM. Thus, the observation of hot stars projected onto the image of the supernova remnant makes it possible to determine the physical conditions and elemental composition by simulating the absorption line profiles in their spectra [166]. Comparing the elemental oxygen content with the water content allows the fraction of oxygen to be directly estimated in water molecules in these regions.

4.3 Water in conditions of extreme star formation

Water formation in central molecular zone. The central molecular zone (CMZ) is a region about 250 pc in size [167] at the center of the Milky Way. This region is characterized by a high gas density of $n > 10^4$ cm^{-3}, velocity dispersion of $\sigma > 10$ km s^{-1}, and complex spatial distribution of molecular gas clouds. These conditions make the CMZ similar to galaxies at high redshifts [168], allowing one to study star formation in the epoch of the young Universe. The total mass of the molecular gas in the CMZ and the star formation rate are estimated from observations as $(3-7) \times 10^7\ M_\odot$ [169] and $0.04-0.4\ M_\odot$ year^{-1} [170, 171]. The star formation rate in the central part of the Galaxy turns out to be almost an order of magnitude higher [172] than the rate that could be expected based on the gas density in the CMZ and the Kennicutt–Schmidt law [173]. An estimate of the star formation rate for the CMZ, based on the count of young stellar objects (bright IR sources), is in the range of $0.05-0.45\ M_\odot$ year^{-1} [174]. Thus, in addition to interest in the physics of processes occurring in such extreme regions as the CMZ, the attention of astrophysicists is also attracted by the observed insufficient star formation rate for such large reserves of molecular hydrogen.

Many observational programs have been devoted to the study of the CMZ, including a spectral survey conducted by the Herschel Space Telescope [175]. Spectra of 49 molecules were obtained in the range from 480 to 1907 GHz in the direction of the Sgr B2 region. This cloud is one of the densest gas–dust complexes in the CMZ, with a size of about 36 pc [176] and a mass of $8 \times 10^6\ M_\odot$. The review revealed absorption lines of ortho- and para-molecules of water H_2O and its isotopologues $H_2^{17}O$ and $H_2^{18}O$, as well as of ortho- and para-molecules H_2O^+; many other oxygen compounds were also reported. The content of oxygen-containing molecules in the direction of Sgr B2 is estimated to be $\sim 3 \times 10^{-7} N_{H_2}$ ($N_{H_2} \approx 3 \times 10^{24}$ cm^{-2} [175]).

Comito et al. [177] showed that water toward the outer shell of Sgr B2 appeared as a result of a high-temperature chain of reactions in the region of shock-wave propagation, while, toward the black hole itself, water was apparently formed on the surfaces of dust particles in a cold environment. To test these assumptions and understand how water was formed in the extreme conditions of the galactic center, it is necessary to determine the fraction of deuterium in this region. If the deuterium fraction is high, water was probably formed in a cold environment, and if the fraction is low, it was formed in a warm environment. Comito et al. [178] also studied the emission lines of heavy water HDO and showed that the HDO content varies by two orders of magnitude, from $\sim 10^{-11}$ to 10^{-9}. Astrochemical simulation in this study did not explain the obtained HDO content, and the absolute values of the water content toward the Sgr B2 core and envelope were found with a large uncertainty [177, 178] due to the significant optical thickness of the water lines and complex line profiles. To remove the uncertainty and estimate the deuterium fraction in the CMZ, observations of optically thin water lines are necessary, which can be done using the Millimetron space observatory.

Water in galaxies with active star formation. The most powerful bursts of star formation are associated with shock waves arising from the merger (collision) of massive galaxies. The late stages of these processes apparently correspond to the bright and ultraluminous infrared galaxies, whose luminosities exceed $10^{11} L_\odot$ and $10^{12} L_\odot$ K, respectively [179]. The prototype of such objects in the local Universe is the galaxy Ar 220, in which two supermassive black holes are surrounded by a huge massive cocoon of gas and dust, including numerous star-forming regions. The interstellar medium in these galaxies is more strongly exposed to the extreme effects of shock waves and ionizing radiation than in most galaxies with 'quiet' star formation, including the Milky Way. In the molecular clouds of the Galaxy, the physical conditions favor the excitation of only the so-called 'low' or 'cold' levels of the water molecule with $E_{up} < 200$ K (see terminology above), with the exception of the vicinity of protostars, where water lines corresponding to highly excited energy levels, among other things, can be detected.

In ultraluminous galaxies, there are conditions for the excitation of numerous 'warm' and 'hot' transitions in water molecules due to powerful star formation, the rate of which is tens and hundreds of times greater than the galactic value, and a high dust content. Similar conditions are realized in central regions of galaxies with a high star formation rate, for example M82; in the vicinity of active galactic nuclei NGC1068, Mrk231, Mrk334, etc. [204, 205]; and in ultraluminous IR galaxies. A significant number of transitions in the water molecule fall within the expected ranges of the instruments of the Millimetron Space Observatory (see Fig. 2). It seems important to obtain estimates of the brightness and spectrally resolved profiles of water lines in a wide frequency range for similar galaxies in the local Universe. Using the obtained estimates of the brightness of the water lines, it is possible to clarify the physical conditions in these objects.

Detection of accompanying chemical components involved in the chemical chains of water formation — in particular, the lines of OH molecules and molecular ions OH^+, H_2O^+, and H_3O^+, observed in the spectra of ultrabright IR galaxies (e.g., [180, 181]), as well as other components, such as CII and CO, falling within the ranges of the instruments of the Millimetron Space Observatory — will further limit the range of physical parameters.

4.4 Water transport in star-forming regions and connection with emergence of life on Earth

Interest in studying the origin of water in protoplanetary disks and comets is associated with the hypothesis of the delivery of water and, possibly, complex organic matter onto Early Earth (see, for example, [182–184]). The boundary of the region of the protosolar disk in which water could condense into solid matter (the so-called water snow line) is located beyond Earth's orbit [185, 186], but there is water on Earth. It is assumed that a source of water molecules could have been cometary meteorite matter during the era of meteorite bombardment of Early Earth. Perhaps this is why oceans formed on Earth. Much less is known about water in the remote parts of protoplanetary disks, where molecules from the primary matter that forms exoplanets survive. It is currently unknown whether the water transfer mechanism worked in the early solar system, what happens in other planetary systems, and to what extent the solar system is unique in the Universe in terms of water distribution [206].

Water in the protoplanetary disk around TW Hya was discovered during Herschel telescope observations in an amount exceeding the mass of Earth's oceans by thousands of times [30]. Two lines of water (ortho and para) were observed during transitions to the ground state. The disk was not spatially resolved, and so the integral characteristics of the theoretical model were compared with the observations. Interestingly, the ortho/para ratio for water in this disk turned out to be ≈ 0.8, which is obviously less than the equilibrium value according to spin statistics and less than that found in solar system comets. The authors concluded that the cometary matter had apparently already been processed during the migration of these bodies through the solar system. The fact that the TW Hya disk contains cold and unrecycled matter can be judged by the deficit of CO molecules frozen into dust, as evidenced by observations with the ALMA interferometer [187]. Spatially resolved ALMA observations of water molecule emission in TW Hya have shown that the inner 17 AU region of the disk contains a water mass that exceeds the mass of Earth's oceans by ≈ 4 times [188]. These observations covered the disk atmosphere, and the data analysis included four excited water lines, using information from previous Herschel observations.

The disks emit not only 'cold' water lines, but also lines corresponding to highly excited transitions, such as vibrational–rotational transitions in the near- and mid-IR, from the inner few AU of the disk [189]. As in molecular clouds, water in the disks should be one of the main coolants, in addition to dust and CO. It is interesting that highly excited transitions of water are also observed in parts of protoplanetary disks distant from the star (JWST observations in [190]), which can be explained by scattering of radiation in lines from the inner parts of the disk by dust particles in the outer parts of the disk. To estimate the mass of water in the inner or outer parts of the disk and to diagnose the physical conditions under which water exists in the disks in the gas phase, samples of disks are needed where highly excited transitions of water are detected and where the Millimetron Space Observatory will detect 'cold' water.

Obviously, these observations are not enough to understand how water is transported in protoplanetary disks and in what quantities the disks contain water. Herschel and later ALMA have captured images of a larger number of protoplanetary disks. Using the ALMA telescope with a resolution of $0.1''$, three emission lines were detected within the protoplanetary disk of V883 Ori: HDO at frequencies of 225 and 241 GHz and $H_2^{18}O$ at 203 GHz [191]. Interestingly, the lines of deuterated water turned out to be brighter than that of the isotopologue $H_2^{18}O$. The radial velocities of these emission lines are consistent with Keplerian rotation in the disk. The emission lines are brightest at a radius of 50 to 60 AU and extend to ~ 160 AU. Tobin et al. [191] came to the conclusion that water in the protoplanetary disk is directly inherited from the protostellar cloud, since the fraction of deuterium in water is $\approx 2.3 \times 10^{-3}$. This water can be found in large bodies, for example, cometary nuclei, without significant chemical changes. The same disk was observed with ALMA in the lines of complex organic molecules — methanol, acetone, acetonitrile, acetaldehyde, and methyl formate [192]. It was shown that the content of these molecules is consistent with their content in cometary matter [193].

Protoplanetary disks are heterogeneous in their properties, and therefore a large number of observations of protoplanetary disks, about 100–1000, are needed to understand which of them contain water and which do not. The issue of how the water content in disks depends on the mass of the star and its environment (UV field, cosmic-ray ionization rate) has not been studied. Interestingly, protoplanetary disks survive even in such extreme conditions as photodissociation regions [194, 195].

In this regard, it seems very important to estimate the total mass of protoplanetary disks, including disks containing water. Since the main component of the gas in disks, molecular hydrogen H_2, does not have emission lines at temperatures corresponding to the physical conditions in dense interstellar clouds in which stars and planets are formed, the mass of H_2 is estimated indirectly: from observations of the CO molecule (most common after H_2), or from observations of dust emission. However, estimates of the mass of protoplanetary disks based on CO and dust are associated with significant inaccuracies, since they are strongly model-dependent.

An alternative method for measuring the mass of disks based on the emission of the isotopologue of molecular hydrogen HD at a wavelength of 112 μm [196] was implemented using Herschel observations, leading to a highly accurate assessment of the masses of two protoplanetary disks; upper limits on the mass were estimated for four disks [197]. It seems important to significantly increase the number of these statistics using observations with the Millimetron Space Observatory in the 2.67-THz range in order to identify patterns in the mass distribution of disks and the relationship with the mass of the water contained in them, as well as to draw conclusions about the evolution of disks during their formation.

Also necessary is an observational study of the positions of snow lines of not only water but also other molecules in disks. For example, Leemker et al. [198] suggested that the water snow line can be traced by observing the emission lines of HCO^+ and $H^{13}CO^+$ molecules with ALMA. By the time the Millimetron Space Observatory is launched, a large volume of ALMA observations of disks will have been accumulated, which will allow astrochemical models to be tested in detail, the number of free parameters in them to be reduced, and the transport of water in disks to be studied.

The question of the connection between the icy nuclei of comets and Earth's oceans still remains open [199]. The key

indicator of the origin of Earth's water is considered to be the relative content of semi-heavy water (HDO) in Earth's oceans, approximately 1.6×10^{-4} [200]. This value is close to the HDO content in carbonaceous chondrites, which led to the assumption that water was delivered to Earth from asteroids rather than from comets. This was also indicated by the HDO content in cometary atmospheres, which was two to three times higher than that in Earth's oceans. However, other geochemical constraints (related to isotopes of other elements) indicate that, in general, the contribution of matter similar to that of carbonaceous chondrites to the total mass of Earth did not exceed a few percent (see, for example, [201]). This means that water from C-class asteroids (related to carbonaceous chondrites) could have been delivered only after the formation of the bulk of Earth. On the other hand, Hartogh et al. [26] indirectly confirmed the idea of the cometary origin of Earth's water, where, based on observations of two lines, HDO $1_{10}-1_{01}$ and $H_2^{18}O$ $1_{10}-1_{01}$, they found that the fraction of deuterium in the coma of comet 103P/Hartley 2 ($\approx 1.6 \times 10^{-4}$) coincides with that found in ocean water. Lis et al. [28] obtained a similar result for the comet 46P/Wirtanen. In addition, Lis et al. [28] suggested that the HDO content in the substance ejected from the cometary nucleus may depend on the comet's activity level and does not necessarily reflect the actual HDO/H_2O ratio in the nucleus. This conclusion, however, contradicts the measurements of the HDO/H_2O ratio near comet 67P/Churyumov–Gerasimenko [202], which showed no dependence on the heliocentric distance or the activity level of the nucleus. Obviously, to solve the problem of the origin of water on Earth, it is necessary to increase the number of comets with measured HDO and H_2O ratios to 100 or more, which has not been done so far and which can be done with the Millimetron Space Observatory.

The scientific novelty of comet studies is that, along with the main ortho-H_2O $1_{10}-1_{01}$ line, the Millimetron Space Observatory will observe isotopologue lines that produce optically thin radiation. The profile of the main line is often distorted due to the self-absorption effect, which does not allow the water content to be accurately determined in an object or the kinematics of the gas in it to be studied; therefore, a transition to mass observations of optically thin radiation is needed. All of the above observations are studies of comets in the single-mirror regime, when both the nucleus and part of the coma fell into the telescope's beam pattern due to its large angular size. Of interest is the mapping of comet comas, which was practically impossible with the Herschel telescope due to its low spatial resolution. Mapping of comas in water lines at 557 GHz was performed only for some comets and made it possible to reveal the anisotropy of the outflow from the coma [203]. Mapping cometary comas in these lines will allow the excitation of transitions to be studied as a function of the direction to the Sun (for example, [31]).

5. Conclusions

We have considered the problems of the formation and transport of water molecules in various space objects: from active galaxies to protoplanetary disks and comets, which is one of the key scientific program of the Millimetron Space Observatory. The main mechanisms of formation and destruction of water molecules in the interstellar medium, molecular clouds, protostellar disks, and supernova remnants have been reviewed. The issues of the formation of water molecules on the surface of dust particles, the transition of molecules from the solid phase to the gas phase, the influence of background radiation and shock fronts in star-forming regions, the transport of molecular gas in the interstellar medium, and outflows from galaxies have been discussed. Note that, to assess the water content in space objects and the physical conditions in them, not only are new observations needed, but so is the development of adequate numerical models. The need to apply a nonequilibrium (non-LTE) approach to the analysis of water molecule emission lines has been emphasized.

Successful implementation of the program will allow us to make a qualitative transition from the available fragmentary information about the water content in individual objects to obtaining statistical patterns of the evolution of the water content in protostellar clouds, protoplanetary disks, and comets and, finally, to come closer to understanding the conditions under which life can arise on planets. Observations of the water line in the local Universe will help answer the question of the universality of the star formation process in galaxies of different types or will reveal specific features associated with the propagation of shock waves in them. To achieve the set objectives, it is planned to use the high-resolution heterodyne spectrometer of the Millimetron Space Observatory, the operating range of which covers the main transitions in the water molecule.

Acknowledgments. The authors thank A.F. Punanova and V.V. Akimkin for useful advice in preparing this paper.

References

1. Kardashev N S et al. *Phys. Usp.* **57** 1199 (2014); *Usp. Fiz. Nauk* **184** 1319 (2014)
2. Novikov I D et al. *Phys. Usp.* **64** 386 (2021); *Usp. Fiz. Nauk* **192** 404 (2021)
3. Likhachev S F, Larchenkova T I *Phys. Usp.* **67** 768 (2024); *Usp. Fiz. Nauk* **194** 814 (2024)
4. Ladeyschikov D A et al. *Astron. J.* **163** 124 (2022)
5. Sanna A et al. *Astrophys. J.* **745** 82 (2012)
6. Reid M J et al. *Astrophys. J.* **885** 131 (2019)
7. Reid M J *Publ. Astron. Soc. Pacific* **134** 123001 (2022)
8. Val'tts I E *Astron. Rep.* **67** 1348 (2023); *Astron. Zh.* **100** 1210 (2023)
9. Reid M J, Pesce D W, Riess A G *Astrophys. J. Lett.* **886** L27 (2019)
10. Volvach A E, Volvach L N, Larionov M G *Mon. Not. R. Astron. Soc.* **507** L52 (2021)
11. Ladeyschikov D A et al. *Astrophys. J. Suppl.* **261** 14 (2022)
12. van Dishoeck E F et al. *Astron. Astrophys.* **648** A24 (2021)
13. Tretyakov I V et al. *IEEE Trans. Terahertz Sci. Technol.* **15** 191 (2025)
14. De Graauw Th et al. *Astron. Astrophys.* **518** L6 (2010)
15. Richards P L et al. *Appl. Phys. Lett.* **34** 345 (1979)
16. Dolan G J, Phillips T G, Woody D P *Appl. Phys. Lett.* **34** 347 (1979)
17. Wootten A, Thompson A R *Proc. IEEE* **97** 1463 (2009)
18. Güsten R et al. *Proc. SPIE* **6267** 626714 (2006)
19. Uzawa Y et al. *Radio Sci.* **56** e2020RS007157 (2021)
20. Khudchenko A et al. *IEEE Trans. Terahertz Sci. Technol.* **9** 532 (2019)
21. Gol'tsman G N et al. *Supercond. Sci. Technol.* **4** 453 (1991)
22. Tretyakov I et al. *Appl. Phys. Lett.* **98** 033507 (2011)
23. Williams B S *Nature Photon.* **1** 517 (2007)
24. Zhao Y et al. *Laser Photon. Rev.* **15** 2000498 (2021)
25. Hayton D J et al. *Appl. Phys. Lett.* **103** 051115 (2013)
26. Hartogh P et al. *Nature* **478** 218 (2011)
27. Lis D C et al. *Astrophys. J. Lett.* **774** L3 (2013)
28. Lis D C et al. *Astron. Astrophys.* **625** L5 (2019)
29. Caselli P et al. *Astrophys. J. Lett.* **759** L37 (2012)
30. Hogerheijde M R et al. *Science* **334** 338 (2011)
31. Bockelée-Morvan D et al. *Astron. Astrophys.* **544** L15 (2012)

32. Kraus J D *Radio Astronomy* (New York: McGraw-Hill, 1966)
33. Kristensen L E et al. *Astron. Astrophys.* **542** A8 (2012)
34. Prasad S S, Huntress W T (Jr.) *Astrophys. J. Suppl.* **43** 1 (1980)
35. Le Teuff Y H, Millar T J, Markwick A J *Astron. Astrophys. Suppl.* **146** 157 (2000)
36. Lamberts T et al. *Phys. Chem. Chem. Phys.* **15** 8287 (2013)
37. van Dishoeck E F, Herbst E, Neufeld D A *Chem. Rev.* **113** 9043 (2013)
38. Solomon P M, Werner M W *Astrophys. J.* **165** 41 (1971)
39. Hollenbach D et al. *Astrophys. J.* **690** 1497 (2009)
40. McClure M K et al. *Nat. Astron.* **7** 431 (2023)
41. Tielens A G G M, Hagen W, Greenberg J M *J. Phys. Chem.* **87** 4220 (1983)
42. Hiraoka K et al. *J. Geophys. Res.* **113** E02013 (2008) https://doi.org/10.1029/2007JE002926
43. Dulieu F et al. *Astron. Astrophys.* **512** A30 (2010)
44. Walmsley C M et al. *Astron. Astrophys.* **364** 301 (2000)
45. Wolfire M G, Vallini L, Chevance M *Annu. Rev. Astron. Astrophys.* **60** 247 (2022)
46. Kirsanova M S et al. *Astrophys. Bull.* **78** 372 (2023); *Astrofiz. Byull.* **78** 389 (2023)
47. Padovani M et al. *Space Sci. Rev.* **216** 29 (2020)
48. Meijerink R, Cazaux S, Spaans M *Astron. Astrophys.* **537** A102 (2012)
49. Dupuy R et al. *Nat. Astron.* **2** 796 (2018)
50. Notsu S et al. *Astron. Astrophys.* **650** A180 (2021)
51. Oba Y et al. *Astrophys. J.* **749** 67 (2012)
52. Lamberts T et al. *Astron. Astrophys.* **570** A57 (2014)
53. Meisner J, Lamberts T, Kästner J *ACS Earth Space Chem.* **1** 399 (2017)
54. Atkinson R et al. *Atmos. Chem. Phys.* **4** 1461 (2004)
55. Vasyunin A I, Herbst E *Astrophys. J.* **769** 34 (2013)
56. Cuppen H M, Karssemeijer L J, Lamberts T *Chem. Rev.* **113** 8840 (2013)
57. Tielens A G G M *Astron. Astrophys.* **119** 177 (1983)
58. Roberts H, Herbst E, Millar T J *Astrophys. J.* **591** L41 (2003)
59. Watson W D *Rev. Mod. Phys.* **48** 513 (1976)
60. Aikawa Y, Herbst E *Astron. Astrophys.* **351** 233 (1999)
61. Taquet V, Charnley S B, Sipilä O *Astrophys. J.* **791** 1 (2014)
62. Furuya K, van Dishoeck E F, Aikawa Y *Astron. Astrophys.* **586** A127 (2016)
63. Prodanović T, Steigman G, Fields B D *Mon. Not. R. Astron. Soc.* **406** 1108 (2010)
64. Lamberts T et al. *Astrophys. J.* **928** 48 (2022)
65. Miyauchi N et al. *Chem. Phys. Lett.* **456** 27 (2008)
66. Ioppolo S et al. *Phys. Chem. Chem. Phys.* **12** 12065 (2010)
67. Oba Y et al. *Astrophys. J.* **701** 464 (2009)
68. Cuppen H M et al. *Phys. Chem. Chem. Phys.* **12** 12077 (2010)
69. Linnartz H, Ioppolo S, Fedoseev G *Int. Rev. Phys. Chem.* **34** 205 (2015)
70. Fraser H J et al. *Mon. Not. R. Astron. Soc.* **327** 1165 (2001)
71. Minissale M et al. *ACS Earth Space Chem.* **6** 597 (2022)
72. Westley M S et al. *Nature* **373** 405 (1995)
73. Öberg K I et al. *Astrophys. J.* **693** 1209 (2009)
74. Fillion J-H et al. *ACS Earth Space Chem.* **6** 100 (2022)
75. Bulak M et al. *Astron. Astrophys.* **677** A99 (2023)
76. Dulieu F et al. *Sci. Rep.* **3** 1338 (2013)
77. Brown W L, Lanzerotti L J, Johnson R E *Science* **218** 525 (1982)
78. Shen C J et al. *Astron. Astrophys.* **415** 203 (2004)
79. Dartois E et al. *Astron. Astrophys.* **576** A125 (2015)
80. Mumma M J, Charnley S B *Annu. Rev. Astron. Astrophys.* **49** 471 (2011)
81. Willacy K et al. *Space Sci. Rev.* **197** 151 (2015)
82. Hama T, Kouchi A, Watanabe N *Science* **351** 65 (2016)
83. Hama T, Kouchi A, Watanabe N *Astrophys. J. Lett.* **857** L13 (2018)
84. Martín-Doménech R et al. *Astron. Astrophys.* **564** A8 (2014)
85. Hiraoka K et al. *Astrophys. J.* **498** 710 (1998)
86. Ioppolo S et al. *Astrophys. J.* **686** 1474 (2008)
87. Jing D et al. *Astrophys. J. Lett.* **741** L9 (2011)
88. Liu L et al. *Astrophys. J.* **846** 5 (2017)
89. Asplund M et al. *Annu. Rev. Astron. Astrophys.* **47** 481 (2009)
90. Przybilla N, Nieva M-F, Butler K *Astrophys. J.* **688** L103 (2008)
91. Meyer D M, Jura M, Cardelli J A *Astrophys. J.* **493** 222 (1998)
92. Whittet D C B *Astrophys. J.* **710** 1009 (2010)
93. Cardelli J A et al. *Astrophys. J. Lett.* **402** L17 (1993)
94. Sofia U J et al. *Astrophys. J.* **605** 272 (2004)
95. Lacy J H et al. *Astrophys. J. Lett.* **428** L69 (1994)
96. Gibb E L et al. *Astrophys. J. Suppl.* **151** 35 (2004)
97. Öberg K I et al. *Astrophys. J.* **740** 109 (2011)
98. Neufeld D A, Kaufman M J *Astrophys. J.* **418** 263 (1993)
99. Neufeld D A, Lepp S, Melnick G J *Astrophys. J. Suppl.* **100** 132 (1995)
100. Rho J et al. *Astrophys. J.* **812** 44 (2015)
101. Sano H et al. *Astrophys. J.* **958** 53 (2023)
102. Wardle M *Astrophys. J.* **525** L101 (1999)
103. Hewitt J W, Yusef-Zadeh F, Wardle M *Astrophys. J.* **683** 189 (2008)
104. Rachford B L et al. *Astrophys. J.* **577** 221 (2002)
105. Shull J M, Danforth C W, Anderson K L *Astrophys. J.* **911** 55 (2021)
106. van Dishoeck E F, Black J H *Astrophys. J.* **334** 771 (1988)
107. Sonnentrucker P et al. *Astrophys. J. Suppl.* **168** 58 (2007)
108. Lambert D L, Sheffer Y, Crane P *Astrophys. J. Lett.* **359** L19 (1990)
109. van Dishoeck E F, Black J H, in *Rate Coefficients in Astrochemistry* (Astrophysics and Space Science Library, Vol. 146, Eds T J Millar, D A Williams) (Dordrecht: Springer, 1988) p. 209, https://doi.org/10.1007/978-94-009-3007-0_14
110. Snow T P (Jr.) *Astrophys. J.* **204** L127 (1976)
111. Spaans M et al. *Astrophys. J.* **503** 780 (1998)
112. Neufeld D A et al. *Astrophys. J.* **580** 278 (2002)
113. Flagey N et al. *Astrophys. J.* **762** 11 (2013)
114. Caselli P et al. *Astrophys. J.* **874** 89 (2019)
115. Schmalzl M et al. *Astron. Astrophys.* **572** A81 (2014)
116. Pavlyuchenkov Ya N, Zhilkin A G *Astron. Rep.* **57** 641 (2013); *Astron. Zh.* **90** 699 (2013)
117. Pavlyuchenkov Ya N et al. *Astron. Rep.* **59** 133 (2015); *Astron. Zh.* **91** 154 (2015)
118. Pavlyuchenkov Ya N, Shustov B M *Astron. Rep.* **48** 315 (2004); *Astron. Zh.* **81** 348 (2004)
119. Pavlyuchenkov Ya et al. *Astrophys. J.* **689** 335 (2008)
120. Bovino S et al. *Astron. Astrophys.* **654** A34 (2021)
121. Wakelam V et al. *Astron. Astrophys.* **647** A172 (2021)
122. Ryabukhina O L et al. *Mon. Not. R. Astron. Soc.* **517** 4669 (2022)
123. Lee C W, Myers P C *Astrophys. J. Suppl.* **123** 233 (1999)
124. McKee C F, Tan J C *Astrophys. J.* **585** 850 (2003)
125. Vázquez-Semadeni E et al. *Astrophys. J.* **657** 870 (2007)
126. Vorobyov E I, Basu S *Astrophys. J.* **633** L137 (2005)
127. Omura M, Tokuda K, Machida M N *Astrophys. J.* **963** 72 (2024)
128. Audard M et al., in *Protostars and Planets VI* (The University of Arizona Space Science Ser., Eds H Beuther et al.) (Tucson, AZ: Univ. of Arizona Press, 2014) p. 387
129. Caratti o Garatti A et al. *Nature Phys.* **13** 276 (2017)
130. Visser R, Bergin E A *Astrophys. J. Lett.* **754** L18 (2012)
131. Vorobyov E I et al. *Astron. Astrophys.* **658** A191 (2022)
132. Houge A, Krijt S *Mon. Not. R. Astron. Soc.* **521** 5826 (2023)
133. Topchieva A et al. *Mon. Not. R. Astron. Soc.* **530** 2731 (2024)
134. Pagani L et al. *Science* **329** 1622 (2010)
135. Dartois E et al. *Nat. Astron.* **8** 359 (2024)
136. Herpin F et al. *Astron. Astrophys.* **587** A139 (2016)
137. Karska A et al. *Astron. Astrophys.* **572** A9 (2014)
138. Bisschop S E et al. *Astron. Astrophys.* **465** 913 (2007)
139. Nesterenok A V *Mon. Not. R. Astron. Soc.* **449** 2875 (2015)
140. Gray M D et al. *Mon. Not. R. Astron. Soc.* **456** 374 (2016)
141. González-Alfonso E et al. *Astron. Astrophys.* **666** L3 (2022)
142. Kraemer K E, Jackson J M, Lane A P *Astrophys. J.* **503** 785 (1998)
143. Schneider N et al. *Astron. Astrophys.* **617** A45 (2018)
144. Larsson B, Liseau R *Astron. Astrophys.* **608** A133 (2017)
145. Kirsanova M S et al. *Mon. Not. R. Astron. Soc.* **497** 2651 (2020)
146. Hollenbach D, McKee C F *Astrophys. J. Suppl.* **41** 555 (1979)
147. Draine B T, Roberge W G, Dalgarno A *Astrophys. J.* **264** 485 (1983)
148. Kaufman M J, Neufeld D A *Astrophys. J.* **456** 250 (1996)
149. Kaufman M J, Neufeld D A *Astrophys. J.* **456** 611 (1996)
150. Flower D R, Pineau des Forêts G *Mon. Not. R. Astron. Soc.* **406** 1745 (2010)
151. Draine B T *Astrophys. J.* **241** 1021 (1980)
152. Godard B et al. *Astron. Astrophys.* **622** A100 (2019)
153. Gusdorf A et al. *Astron. Astrophys.* **532** A53 (2011)

154. Flower D R, Pineau des Forêts G *Mon. Not. R. Astron. Soc.* **268** 724 (1994)
155. Jiménez-Serra I et al. *Astron. Astrophys.* **482** 549 (2008)
156. San José-García I et al. *Astron. Astrophys.* **585** A103 (2016)
157. Kaufman M J, Neufeld D A *Astrophys. J.* **456** 250 (1996)
158. Hollenbach D, Elitzur M, McKee C F *Astrophys. J.* **773** 70 (2013)
159. Molinari S et al. *Astron. Astrophys.* **518** L100 (2010)
160. Schuller F et al. *Astron. Astrophys.* **504** 415 (2009)
161. Zhou P et al. *Astrophys. J.* **826** 34 (2016)
162. Chiotellis A, Schure K M, Vink J *Astron. Astrophys.* **537** A139 (2012)
163. Ranasinghe S, Leahy D *Astrophys. J. Suppl.* **265** 53 (2023)
164. Reach W T, Rho J *Astrophys. J.* **507** L93 (1998)
165. Snell R L et al. *Astrophys. J.* **620** 758 (2005)
166. Ritchey A M et al. *Astrophys. J.* **897** 83 (2020)
167. Morris M, Serabyn E *Annu. Rev. Astron. Astrophys.* **34** 645 (1996)
168. Kruijssen J M D, Longmore S N *Mon. Not. R. Astron. Soc.* **435** 2598 (2013)
169. Ferrière K, Gillard W, Jean P *Astron. Astrophys.* **467** 611 (2007)
170. Immer K et al. *Astron. Astrophys.* **548** A120 (2012)
171. Longmore S N et al. *Mon. Not. R. Astron. Soc.* **429** 987 (2013)
172. Barnes A T et al. *Mon. Not. R. Astron. Soc.* **469** 2263 (2017)
173. Kennicutt R C (Jr.) *Astrophys. J.* **498** 541 (1998)
174. Hatchfield H P et al. *Astrophys. J.* **962** 14 (2024)
175. Möller T et al. *Astron. Astrophys.* **651** A9 (2021)
176. Schmiedeke A et al. *Astron. Astrophys.* **588** A143 (2016)
177. Comito C et al. *Astron. Astrophys.* **402** 635 (2003)
178. Comito C et al. *Astron. Astrophys.* **521** L38 (2010)
179. Sanders D B, Mirabel I F *Annu. Rev. Astron. Astrophys.* **34** 749 (1996)
180. Rangwala N et al. *Astrophys. J.* **743** 94 (2011)
181. González-Alfonso E et al. *Astron. Astrophys.* **550** A25 (2013)
182. Chyba C F et al. *Science* **249** 366 (1990)
183. Marty B *Earth Planet. Sci. Lett.* **313–314** 56 (2012)
184. Ehrenfreund P, Charnley S B *Annu. Rev. Astron. Astrophys.* **38** 427 (2000)
185. Harsono D, Bruderer S, van Dishoeck E F *Astron. Astrophys.* **582** A41 (2015)
186. Wiebe D S et al. *Mon. Not. R. Astrophys. Soc.* **485** 1843 (2019)
187. Nomura H et al. *Astrophys. J.* **914** 113 (2021)
188. Facchini S et al. *Nat. Astron.* **8** 587 (2024)
189. Carr J S, Tokunaga A T, Najita J *Astrophys. J.* **603** 213 (2004)
190. Arulanantham N et al. *Astrophys. J. Lett.* **965** L13 (2024); arXiv:2402.12256
191. Tobin J J et al. *Nature* **615** 227 (2023)
192. Lee J-E et al. *Nat. Astron.* **3** 314 (2019)
193. Le Roy L et al. *Astron. Astrophys.* **583** A1 (2015)
194. Haworth T J et al. *Mon. Not. R. Astron. Soc.* **525** 4129 (2023)
195. Berné O et al., PDRs4All Team *Science* **383** 988 (2024)
196. Bergin E A et al. *Nature* **493** 644 (2013)
197. McClure M K et al. *Astrophys. J.* **831** 167 (2016)
198. Leemker M et al. *Astron. Astrophys.* **646** A3 (2021)
199. O'Brien D P et al. *Space Sci. Rev.* **214** 47 (2018)
200. Hagemann R, Nief G, Roth E *Tellus* **22** 712 (1970) https://doi.org/10.1111/j.2153-3490.1970.tb00540.x
201. Burkhardt C et al. *Sci. Adv.* **7** eabj7601 (2021)
202. Müller D R et al. *Astron. Astrophys.* **662** A69 (2022)
203. Biver N et al. *Planet. Space Sci.* **55** 1058 (2007)
204. González-Alfonso E et al. *Astron. Astrophys.* **561** A27 (2014)
205. Smirnova A, Moiseev A *Mon. Not. R. Astron. Soc.* **401** 307 (2010)
206. Wiebe D Z et al. *Astron. Rep.* **52** 976 (2008); *Astron. Zh.* **85** 1086 (2008)